Exoplanetary radio emission under different stellar wind conditions

Jean-Mathias Griessmeier, S. Preusse, Maxim L. Khodachenko, U. Motschmann, Gottfried Mann, Helmut O. Rucker

Available online at www.sciencedirect.com
ScienceDirect
Planetary and Space Science 55 (2007) 618–630
Planetary and Space Science
www.elsevier.com/locate/pss

Exoplanetary radio emission under different stellar wind conditions

J.-M. Grießmeier[a,b,*,1], S. Preusse[c], M. Khodachenko[d], U. Motschmann[a], G. Mann[e], H.O. Rucker[d]

[a]*Technische Universität Braunschweig, Mendelssohnstraße 3, 38106 Braunschweig, Germany.*
[b]*LESIA, CNRS-Observatoire de Paris, 92195 Meudon, France*
[c]*Max-Planck Institut für Sonnensystemforschung, Max-Planck-Straße 2, 37191 Katlenburg-Lindau, Germany*
[d]*Institut für Weltraumforschung, Österreichische Akademie der Wissenschaften, Schmiedlstrasse 6, 8042 Graz, Austria*
[e]*Astrophysikalisches Institut Potsdam, An der Sternwarte 16, 14482 Potsdam, Germany*

Received 5 December 2005; accepted 27 January 2006
Available online 31 October 2006

Abstract

Radio emission from extrasolar giant planets in close orbits around their host star is an active field of research, including both observational efforts and theoretical work aiming at reasonable predictions for different target planets. So far, most theoretical work assumed a distance-independent, constant stellar wind velocity. This approach is improved and expanded in two respects: first, from stellar wind models, it is known that at close distances the stellar wind is still slow and has not yet reached the velocity it has at larger distances. For this reason, less energy is available for the generation of planetary radio emission than predicted by simplified models. This correspondingly reduces the intensity of stellar wind-driven planetary radio emission, which is calculated taking into account the stellar age. Second, it can be shown that under certain conditions the steady stellar wind has to be replaced by stellar coronal mass ejections. In those cases, the planetary radio flux is strongly increased. The different flux levels expected for planets subject to different stellar wind conditions are analyzed and compared. In addition, different uncertainties in this radio flux estimation are calculated and discussed.

Keywords: Exoplanets; Planetary radio emission; Magnetic moments; Stellar coronal mass ejections

1. Introduction

All strongly magnetized planets in the solar system are known to be sources of nonthermal radio emission. Planetary radio emission is caused by the cyclotron maser instability (for a review, see Zarka, 1998). For giant gaseous extrasolar planets with small orbital distances (the class of "Hot Jupiters"), much stronger radio emission is expected than for the solar system planets (Zarka et al., 1997, 2001; Farrell et al., 1999, 2004; Lazio et al., 2004; Stevens, 2005; Grießmeier et al., 2005). Different studies show that planetary decametric radio emission can be expected to exceed the emission of the planetary host star (Zarka et al., 1997; Grießmeier et al., 2005), and indicate that such planetary emission will be detectable from the ground in the near future (see, e.g. Farrell et al., 2004; Zarka, 2004; Grießmeier et al., 2006a). In the case of the detection of a radio signal, it will be necessary to discriminate the planetary radio emission from that of its host star. This can be achieved in several ways. Firstly, planetary radio emission is strongly polarized (Zarka, 1998), which is not the case for most components of the solar radio emission (see Grießmeier et al., 2005, for a comparison). Secondly, the bursty component could possibly be discriminated by occultation during secondary eclipses. Thirdly, the bursty emission is expected to show some periodicity with either the stellar or planetary rotation according to its origin.

So far, most theoretical work on planetary radio emission was based on a highly simplified treatment of the stellar wind. In this picture, the stellar wind velocity has a constant value, which does not depend either on time or

*Corresponding author. Technische Universität Braunschweig, Mendelssohnstraße 3, 38106 Braunschweig, Germany.
E-mail address: j-m.griessmeier@tu-bs.de (J.-M. Grießmeier).
[1]Current address. LESIA, CNRS-Observatoire de Paris, 92195 Meudon, France.

0032-0633/$ - see front matter © 2006 Elsevier Ltd. All rights reserved.
doi:10.1016/j.pss.2006.01.008

location. Grießmeier et al. (2005) showed that the evolution of the stellar wind on large timescales has to be taken into account, but still assumed the stellar wind to be constant on short timescales. Also, the stellar wind velocity was assumed to be independent of orbital distance (this simplification is hereafter denoted as "simplified stellar wind model"). It is known, however, that at close distances the stellar wind velocity has not yet reached the value it has at larger orbital distances. For this reason, the simplified stellar wind model overestimates the amount of energy available for the generation of planetary radio emission. Within this work, these calculations will be refined and revised using a stellar wind model which takes into account the dependence of stellar wind velocity from stellar distance.

In addition, it can be shown that for stars with frequent enough stellar coronal mass ejections (CMEs) similar to solar CMEs, these CMEs affect exoplanets not as transient events (as is the case for solar CMEs and the solar system planets), but exert their influence continuously. In such a case, the steady stellar wind is effectively replaced by a stream of stellar CMEs. The influence of such stellar CMEs on extrasolar planets is currently under discussion. Different effects were suggested, as, for example, the possible increase of atmospheric loss caused by CMEs (Khodachenko et al., 2006a,b), or the influence of impacting CMEs on the intensity of planetary radio emission (Grießmeier et al., 2006b). The latter effect is put into a more general context here.

In this work, the different radio flux density levels expected for planets subject to various stellar wind conditions are analyzed and compared. We consider parameters obtained for (a) distance-dependent stellar winds of stars of different ages and (b) conditions typical for CMEs. Using the planet τ Bootes b as an example, we discuss the expected influence of the different stellar wind conditions on planetary radio emission. Also, different uncertainties in the radio flux estimation are calculated and discussed.

This paper is organized as follows: Section 2 describes the steady stellar wind model used in this work. Typical properties of CMEs are presented in Section 3. The size of the magnetosphere resulting from the two different types of interaction is calculated in Section 4. The radio fluxes expected for different situations and their uncertainties are computed and compared in Section 5. Section 6 closes with a few concluding remarks.

2. Stellar wind

It is known that at the close orbital distances of Hot Jupiters the stellar wind has not yet reached the quasi-asymptotic velocity regime. In many cases, the stellar wind velocity is even below the Alfvén velocity (Preusse et al., 2005; Erkaev et al., 2005; Preusse, 2006). Because of the low stellar wind velocity, less energy is available for the generation of planetary radio emission than one would expect from more simplified stellar wind models. For this reason, a model with a radially dependent stellar wind velocity is required to correctly describe the interaction of close-in exoplanets with their surrounding.

2.1. Choice of model

There are different possibilities to describe a radially dependent stellar wind. For slowly rotating stars, the stellar wind may be described by the solution of the purely hydrodynamic, isothermal model of Parker (1958). In accordance with the observations, this model describes a solar wind with low velocity and large acceleration near the Sun, whereas at larger distances the velocity is large and the acceleration strongly decreases. Quantitatively, this model was shown to be consistent with observed values for the solar wind for regions not too far away from the Sun (Mann et al., 1999).

In the case of strongly magnetized and rapidly rotating stars, it is necessary to use the extended model of Weber and Davis (1967), which includes the centrifugal force due to the stellar rotation and the Lorentz force due to the stellar magnetic field. Preusse et al. (2005, Fig. 2) show that for a star with a rotation period of 30 days, the results of the Parker model (i.e. without rotation) and those of the Weber and Davis model (i.e. with rotation) are indistinguishable. On the other hand, for rotation periods of 3 days, the two models produce stellar wind velocities v differing by a factor of up to two in certain cases (Preusse et al., 2005, Fig. 2). The influence of rotation and Lorentz force on the acceleration of the stellar wind depends on the stellar parameters. For this reason, it has to be checked which model is appropriate here.

Current estimates for stellar wind properties are only valid for stellar ages $\geqslant 0.7$ Gyr (Wood et al., 2005). For a given stellar age t, the stellar rotation period P_{rot} can be calculated (Newkirk, 1980):

$$P_{\mathrm{rot}} \propto \left(1+\frac{t}{\tau}\right)^{0.7}, \tag{1}$$

where the time constant τ is given by $\tau = 2.56 \times 10^7$ yr (calculated from Newkirk, 1980). Comparing this to the solar values of $t_\odot = 4.6$ Gyr and $P_{\mathrm{rot},\odot} = 25.5$ days, the rotation period of a 0.7 Gyr star is found to be 7 days. With the procedure described in Section 2.5, this rotation period combined with the stellar mass of 1.42 solar masses and a radius of 1.48 solar radii for τ Bootes (Fuhrmann et al., 1998) yields a coronal temperature of $T = 2.8 \times 10^6$ K and a particle flux of $F = 4.6 \times 10^{36}\,\mathrm{s}^{-1}$. In order to investigate the validity of the Parker model in comparison with the Weber and Davis model, the stellar magnetic field is scaled according to

$$B_\star = B_\odot \frac{P_{\mathrm{rot},\odot}}{P_{\mathrm{rot},\star}}, \tag{2}$$

i.e. proportional to the ratio of the rotation period $P_{\mathrm{rot},\odot}$ of the Sun to the stellar rotation period $P_{\mathrm{rot},\star}$

(Collier Cameron and Jianke, 1994; Preusse, 2006). The long-term mean solar wind has a particle density of $6.59 \times 10^6\,\mathrm{m}^{-3}$ and an average stellar wind velocity of 425 km/s at 1 AU (Schwenn, 1990). Taking into account a rotation period of 25.5 days and an average radial magnetic field strength of ~3.1 nT at 1 AU, Preusse et al. (2005) thus obtain $B_\odot = 1.435 \times 10^{-4}\,\mathrm{T}$ as a reference magnetic field strength at the solar surface. Thus, for rotation periods $\geqslant 7$ days, we obtain stellar magnetic fields of $B_\star \leqslant 5.2 \times 10^{-4}\,\mathrm{T}$. To find an upper limit for the influence of the stellar magnetic field, we will use this value in the Weber and Davis model.

The stellar wind velocities v are calculated according to the model of Weber and Davis for hypothetical rotation periods ranging from 7 to 30 days, keeping T, F and $B_\star$ fixed to the value corresponding to this star at 0.7 Gyr. For the details of the numerical calculation confer Preusse et al. (2005). The results are shown in Fig. 1 for the location of τ Bootes b (i.e. at 0.0489 AU). The solid line shows the radial velocity component. The inclusion of stellar rotation in the Weber and Davis model introduces an azimuthal velocity component in addition to the radial component. The dashed line shows the total velocity, which is slightly larger than the radial component alone. In the limit of large rotation periods, the solution of the stellar wind model of Parker (dotted line) is recovered. This model will be presented in more detail in Section 2.2. In Fig. 1 it can be seen that for the star τ Bootes, even in the case of a strong stellar magnetic field ($B_\star = 5.2 \times 10^{-4}\,\mathrm{T}$), the influence of the stellar rotation period on the stellar wind velocity is negligible at the location of the planet (i.e. at 0.0489 AU) as the rotation period is required to be larger than 7 days (note that the y-scale starts at 511 km/s). Apparently, for stars similar in mass and radius to τ Bootes and with an age of $\geqslant 0.7$ Gyr, it is sufficient to use the stellar wind model of Parker (1958), and the stellar wind model of Weber and Davis (1967) is not required.

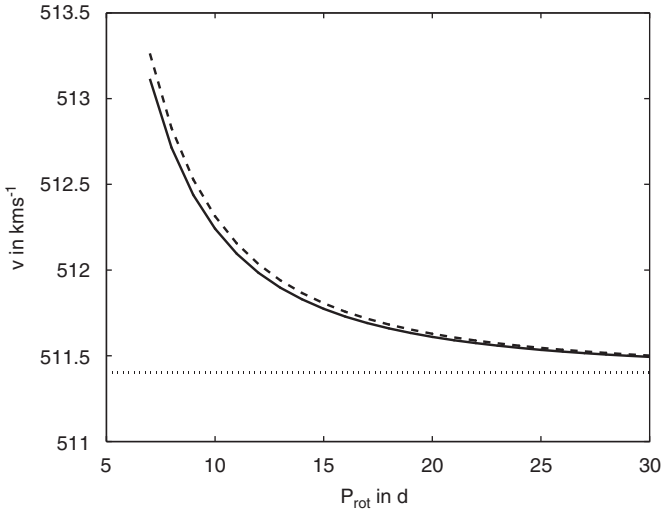

Fig. 1. Stellar wind velocities for τ Bootes at a distance of 0.0489 AU for different stellar rotation periods according to the Weber and Davis stellar wind model (assuming a stellar surface magnetic field of $B_\star = 5.2 \times 10^{-4}\,\mathrm{T}$). The solid line shows the radial component only, whereas the dashed line represents the total velocity. The dotted line represents the Parker limit.

2.2. Radial dependence

As was shown, the radial dependence of the stellar wind properties can be described by the stellar wind model of Parker (1958). In this model, the interplay between stellar gravitation and pressure gradients leads to a supersonic gas flow for sufficiently large substellar distances d (i.e. beyond the *critical radius* defined below). The derivation of *Parker's wind equation*, Eq. (3), can be found in the original work by Parker (1958), in more recent research work (e.g. Mann et al., 1999; Preusse, 2006) or in various textbooks (e.g. Prölss, 2004). It is usually written in the form

$$\frac{v(d)^2}{v_\mathrm{c}^2} - \ln\left(\frac{v(d)^2}{v_\mathrm{c}^2}\right) = 4\ln\frac{d}{r_\mathrm{c}} + 4\,\frac{r_\mathrm{c}}{d} - 3. \tag{3}$$

Here, v_c denotes the critical velocity defined by

$$v_\mathrm{c} = \sqrt{\frac{k_\mathrm{B}T}{m}}, \tag{4}$$

and r_c is the critical radius given by

$$r_\mathrm{c} = \frac{mGM_\star}{4k_\mathrm{B}T}. \tag{5}$$

Furthermore, k_B denotes Boltzmann's constant, T is the temperature of the stellar wind (which is constant and equal to the corona temperature T_corona in this isothermal model), m is the mass of a stellar wind proton, G is the constant of gravitation and $M_\star$ is the stellar mass. For a given distance d, the stellar wind velocity is given by the numerical solution of Eq. (3) which passes through v_c for r_c (i.e. with $v(d = r_\mathrm{c}) = v_\mathrm{c}$). The velocity profile thus is determined by the choice of the coronal temperature T_corona. The stellar mass loss $\dot{M}_\star = 4\pi d^2 nvm$ is the second free parameter. Once it is found, the density profile $n(d)$ can be obtained from the conservation of mass. The T_corona and $\dot{M}_\star$ are determined in the next section.

2.3. Long-term time dependence

Stellar mass loss is a function of the stellar age. The corresponding dependence of the stellar wind parameters n and v on the age of the star is an important ingredient for the estimation of exoplanetary radio emission.

The age dependence of the stellar mass loss rate was found by comparing the astrospheric absorption of stars with different ages. In the region between the astropause and the astrospheric bow shock (analogs to the heliopause and the heliospheric bow shock of the solar system), the partially ionized local interstellar medium (LISM) is heated and compressed. Through charge exchange processes, a population of neutral hydrogen atoms with high temperature is created. The characteristic Lyα absorption (at 1216 Å) of this population was detectable with the

high-resolution observations obtained by the Hubble Space Telescope (HST). The amount of absorption depends on the size of the astrosphere, which is a function of the stellar wind characteristics. Comparing the measured absorption to that calculated by hydrodynamic codes, these measurements allowed the first empirical estimation of the evolution of the stellar mass loss rate as a function of stellar age (Wood et al., 2002, 2005; Wood, 2004).

Similar to Grießmeier et al. (2004) and Lammer et al. (2004), from these observations, and using the results of Newkirk (1980) for the stellar wind velocity, one obtains the time dependence of both the stellar wind velocity and density:

$$v(1\,\mathrm{AU}, t) = v_0\left(1+\frac{t}{\tau}\right)^{-0.43}. \tag{6}$$

The particle density can be determined to be

$$n(1\,\mathrm{AU}, t) = n_0\left(1+\frac{t}{\tau}\right)^{-1.86\pm0.6}. \tag{7}$$

Note that these relations are reliable only for main sequence stars with a stellar age of at least 0.7 Gyr (Wood et al., 2005). The proportionality constants are determined by the present-day conditions. In accordance with Mann et al. (1999), the current stellar wind parameters are taken from the long-term averages of Schwenn (1990), with $v(1\,\mathrm{AU}) = 425\,\mathrm{km/s}$ and $n(1\,\mathrm{AU}) = 6.59\times10^6\,\mathrm{m^{-3}}$ for $t = 4.6\,\mathrm{Gyr}$. This results in $v_0 = 3971\,\mathrm{km/s}$ and $n_0 = 1.04\times10^{11}\,\mathrm{m^{-3}}$ for the nominal case (v_0 and n_0 depend on the exponents of Eqs. (6) and (7)). This revised choice of constants and exponents in Eqs. (6) and (7) supercedes the values adopted by Grießmeier et al. (2004, 2005) and Lammer et al. (2004), who used exponents of -0.4 and -1.5 for $v(t)$ and $n(t)$. The main reason for this modification is that the values of Wood et al. (2002) were replaced by the more precise measurements of Wood et al. (2005). The time constant is $\tau = 2.56\times10^7\mathrm{yr}$ (calculated from Newkirk, 1980). For distances other than 1 AU, $v(d)$ and $n(d)$ have to be calculated according to Section 2.2, choosing T_{corona} and $\dot{M}_\star$ such that at 1 AU both v and n are consistent with the results from Eqs. (6) and (7).

The influence of the time dependence of stellar wind conditions on the expected radio flux from extrasolar planets was discussed by Grießmeier et al. (2005). In Section 5.2, these calculations are refined and updated.

2.4. Influence of orbital motion

For planets at small orbital distances, the keplerian velocity of the planet moving around its star becomes comparable to the stellar wind velocity presented in the previous sections. Thus, the interaction of the stellar wind with the planetary magnetosphere should be calculated using the effective velocity of the stellar wind plasma relative to the planet, which takes into account this "aberration effect" (Zarka et al., 2001).

For the small orbital distances relevant for Hot Jupiters, the planetary orbits are circular because of tidal dissipation. For circular orbits, the orbital velocity v_{kepler} is perpendicular to the stellar wind velocity v, and its value is given by Kepler's law:

$$v_{\mathrm{kepler}} = \omega_{\mathrm{kepler}} d = \sqrt{\frac{M_\star G}{d}}. \tag{8}$$

In the reference frame of the planet, the stellar wind velocity then is given by

$$v_{\mathrm{eff}} = \sqrt{v_{\mathrm{kepler}}^2 + v^2}. \tag{9}$$

As can be seen in Table 1, v_{eff} may differ considerably from v. This is especially true close to the star when v is small.

2.5. Results for density, velocity and temperature

The procedure to obtain the stellar wind velocity $v_{\mathrm{eff}}(d, t, M_\star, R_\star)$ and density $n(d, t, M_\star, R_\star)$ at the location of an exoplanet (i.e. at distance d) for a host star of given age t, mass $M_\star$ and radius $R_\star$ consists of the following:

(i) For a prescribed stellar age, the corresponding values of the stellar wind velocity $v(t, 1\,\mathrm{AU}, M_\odot, R_\odot)$ and stellar wind density $n(t, 1\,\mathrm{AU}, M_\odot, R_\odot)$ at 1 AU are obtained from Eqs. (6) and (7), respectively. From these quantities, the stellar mass loss $\dot{M}_\odot$ is calculated as

$$\dot{M}_\odot(t) = 4\pi d_0^2\, n(d_0) v(d_0) m, \tag{10}$$

where $d_0 = 1\,\mathrm{AU}$.

(ii) In analogy to Eq. (10), one finds $\dot{M}_\star(t) = 4\pi R_\star^2\, n(R_\star) v(R_\star) m$. Thus, the stellar mass loss rate (and in consequence also the stellar wind density) are proportional to the stellar surface area. For this reason, the stellar mass loss has to be calculated from the stellar mass loss obtained in step (i) by

$$\dot{M}_\star(t) = \dot{M}_\odot(t)\frac{R_\star^2}{R_\odot^2}, \tag{11}$$

where $R_\star$ is taken from observations (see Table 2).

(iii) Rather than assume a stellar wind velocity v independent of d, and a stellar wind density n that quadratically decreases with distance (i.e. $n(d) \propto d^{-2}$), as was frequently done before (e.g. Farrell et al., 1999, 2004; Grießmeier et al., 2004, 2005; Lazio et al., 2004), a Parker-like stellar wind model is used to find $n(d)$ and $v(d)$ as a function of the distance to the star. Following the procedure of Section 2.2, the coronal temperature T_{corona} is adjusted until the stellar wind velocity at 1 AU corresponds to the value which was obtained in step (i). With this value of T_{corona}, v can be determined for any value of d by solving Eq. (3). Note that Eq. (3) has more than one solution, of which only one is physically meaningful. At this

Table 1
Age t, stellar wind parameters (density, velocity and temperature), magnetospheric standoff distances R_s (in planetary radii), estimated radio power P_{rad}, estimated flux density at a distance of 1 AU (Φ_{AU}) and at distance s (Φ_s), and maximum emission frequency f_c^{max} are given for different stellar wind situations

Planet	Case	t (Gyr)	n (m^{-3})	v (km/s)	v_{eff} (km/s)	T (MK)	R_s (R_p)	P_{rad} (10^{14} W)	Φ_{AU} (10^{10} Jy)	Φ_s (mJy)	f_c^{max} (MHz)
Jupiter	–	4.6	2.0×10^5	520	520	0.8	40	0.002	0.002	–	23.9
τ Bootes b	REF = SW2.4	2.4	4.9×10^{10}	230	280	1.4	4.6	1.5	4.0	3.9	10.5
τ Bootes b	SSW2.4	2.4	2.0×10^{10}	560	580	–	4.3	7.5	20	19	10.5
τ Bootes b	SW1.0	1.0	2.0×10^{11}	410	440	2.4	3.2	11	30	29	10.5
τ Bootes b	SW4.6	4.6	1.9×10^{10}	140	210	0.9	5.9	0.4	1.1	1.0	10.5
τ Bootes b	CME	–	6.1×10^{10}	500	530	2.0	3.7	7.8	21	20	10.5

The influence of the stellar wind model is seen by comparing the cases SW2.4 (the reference case, also denoted by REF) and SSW2.4 (using the simplified stellar wind model). The importance of the stellar age can be seen by comparing the cases SW1.0, SW2.4 and SW4.6. The influence of stellar coronal mass ejections is found by comparing the cases SW2.4 and SW4.6 to the case CME.

Table 2
Distance from the solar system s, stellar and planetary radius and mass, orbital distance d and the expected planetary magnetic moment $\mathcal{M}$ for Jupiter and for τ Bootes b

Planet	s (pc)	$R_\star$ ($R_\odot$)	$M_\star$ ($M_\odot$)	d (AU)	R_p (R_J)	M_p (R_J)	$\mathcal{M}$ ($\mathcal{M}_J$)
Jupiter	–	1.0	1.0	5.2	1.0	1.0	1.0
τ Bootes b	15.6[a]	1.48[b]	1.42[b]	0.0489[a]	1.2[c]	4.4[c]	0.76

Values taken from: [a] Leigh et al. (2003), [b] Fuhrmann et al. (1998), [c] see text.

point, care must be taken to ensure the correct solution is found (i.e. the solution in which $v(d)$ is monotonically increasing and which reaches 425 km/s at $d = 1$ AU for a star of 4.6 Gyr age). Thus, $v(d,t)$ is obtained.

(iv) The density $n(d,t)$ is then obtained by dividing the stellar mass loss $\dot{M}_\star(t)$ obtained in step (ii) by $4\pi d^2\, v(d) m$, where $v(d,t)$ was obtained in step (iii).

(v) Finally, the stellar wind velocity $v(d,t)$ obtained in step (iii) is replaced by the effective velocity v_{eff} given by Eq. (9).

Unfortunately, there is no closed analytical form for the resulting functions $n(d)$ and $v(d)$. Table 1 gives the resulting stellar wind parameters for different cases. For all the cases of Table 1, v_{eff} is higher than the Alfvén velocity. Also note that the age of τ Bootes is estimated to be approximately 2.4 Gyr (Saffe et al., 2005), so that the 4.6 Gyr case is not realistic for this planet. It is presented here to demonstrate the influence of the stellar system age.

Also note that for G stars, some change in stellar radius is expected during the stellar evolution (Guinan and Ribas, 2002, Fig. 1). This effect was neglected in the calculations.

3. Stellar CMEs

Recently, stellar CMEs similar to solar CMEs were suggested to have a strong influence on close-in extrasolar planets. Both the plasma velocity and density are considerably higher during a CME than for the quiet stellar wind, so that more energy is available for planetary radio emission. In addition, at the close orbital distance of Hot Jupiters, stellar CMEs are expected to impact on a planet much more frequently than in the solar system.

3.1. Results for density, velocity and temperature

In this section, typical properties for CMEs are presented. Of course, not all CMEs have the same properties. Combining a large set of observations, Khodachenko et al. (2006a) derived the dependence of the *average* CME density n_{CME} and of the *average* CME velocity v_{CME} on the substellar distance d.

The current knowledge on CMEs was obtained by studying the Sun. Different observational data on CMEs are available for two distinct spatial domains: (a) the near-Sun region (with $d \leqslant 0.14$ AU), where remote observations were obtained by coronagraphs (i.e. the Large Angle and Spectrometric Coronagraph LASCO on board of ESA's Solar and Heliospheric Observatory SoHO) and (b) the region where data were obtained by in situ observations from various spacecraft (for $d \geqslant 0.3$ AU). With a large database of observations, statistical studies of solar CMEs have been made possible. Connecting the results of remote estimations of the CME parameters near the Sun with those measured in situ at larger distances, Khodachenko et al. (2006a) give two interpolated limiting cases, denoted as *weak* and *strong* CMEs, respectively. These two classes

have a different dependence of the average density on the distance to the Sun d. In the following, these quantities will be labeled $n^{w}_{CME}(d)$ and $n^{s}_{CME}(d)$, respectively.

For weak CMEs, the density $n^{w}_{CME}(d)$ behaves as

$$n^{w}_{CME}(d) = n^{w}_{CME,0}(d/d_0)^{-2.3}, \quad (12)$$

where the density at $d_0 = 1\,\mathrm{AU}$ is given by $n^{w}_{CME,0} = n^{w}_{CME}(d = d_0) = 4.9 \times 10^6\,\mathrm{m}^{-3}$.

For strong CMEs, Khodachenko et al. (2006a) find

$$n^{s}_{CME}(d) = n^{s}_{CME,0}(d/d_0)^{-3.0}, \quad (13)$$

with $n^{s}_{CME,0} = n^{s}_{CME}(d = d_0) = 7.1 \times 10^6\,\mathrm{m}^{-3}$, and $d_0 = 1\,\mathrm{AU}$.

As far as the CME velocity is concerned, one has to note that individual CMEs have very different velocities. However, the *average* CME velocity v is approximately independent of the subsolar distance, and is similar for both types of CMEs:

$$v^{w}_{CME} = v^{s}_{CME} = v_{CME} \approx 5.0 \times 10^5\,\mathrm{m/s}. \quad (14)$$

Similarly to Section 2.4, the CME velocity given by Eq. (14) has to be corrected for the orbital motion of the planet:

$$v_{eff,CME} = \sqrt{\frac{M_\star G}{d} + v^2_{CME}}. \quad (15)$$

In addition to the density and the velocity, the temperature of the plasma in a CME will be required for the calculation of the size of the magnetosphere (Section 4). According to Khodachenko et al. (2006a,b), the front region of a CME consists of hot, coronal material ($T \approx 2\,\mathrm{MK}$). This region may either be followed by relatively cool prominence material ($T \approx 8000\,\mathrm{K}$), or by hot flare material ($T \approx 10\,\mathrm{MK}$). In the following, the temperature of the leading region of the CME will be used, i.e. $T_{CME} = 2\,\mathrm{MK}$.

The values obtained using Eqs. (13)–(15) for the plasma density and velocity during strong CMEs and the corresponding values for the steady stellar wind are compared in Table 1.

3.2. Occurrence rate

In the solar system, impacts of CMEs on a planet occur only very rarely. For close-in extrasolar planets, however, Khodachenko et al. (2006a) find that CME–planet collisions can be expected to happen much more frequently. In some cases, planets may even be under the continuous influence of CMEs.

The argumentation is as follows (Khodachenko et al., 2006a): a CME of angular size Δ_{CME} is assumed to propagate strictly radially from its star. The range of latitudes where CMEs occur is restricted to $\pm\Theta$ around the equatorial plane of the star. Then, the frequency f_{impact} at which CMEs impact on a planet of an angular size δ_p can be estimated to be (Khodachenko et al., 2006a)

$$f_{impact} = \frac{(\Delta_{CME} + \delta_p)\sin((\Delta_{CME} + \delta_p)/2)}{2\pi \sin\Theta} f_{CME}, \quad (16)$$

where f_{CME} is the frequency with which CMEs are ejected by the star, and the coefficient in front of f_{CME} describes the probability for an ejected CME to collide with the planet. A planet can be assumed to be under the permanent influence of CMEs when the time between two successive CME impacts is shorter than the duration of a CME collision. In other words, the CME impact rate has to exceed a critical level given by

$$f_{impact} \geqslant \frac{1}{\tau_{CME}}, \quad (17)$$

where τ_{CME} is the duration of the CME (due to its three-dimensional structure travelling across the planetary location).

From Eqs. (16) and (17), one can estimate the critical CME production rate f^{c}_{CME}:

$$f^{c}_{CME} = \frac{2\pi \sin\Theta}{(\Delta_{CME} + \delta_p)\sin((\Delta_{CME} + \delta_p)/2)\tau_{CME}}. \quad (18)$$

If the stellar CME production rate exceeds f^{c}_{CME}, then the discrete character of CME–planet encounters is replaced by a continuous influence: to obtain an estimation for the value of f^{c}_{CME}, stellar CMEs are assumed to be similar to solar CMEs, i.e. $\pi/3 \leqslant \Delta_{CME} \leqslant 2\pi/3$ and $\tau_{CME} \approx 8\,\mathrm{h}$ (full width at half maximum of the measured brightness at heliocentric distances of 6–10 solar radii, see Lara et al., 2004). Furthermore, the angular size of the planet is neglected ($\delta_p \to 0$), and CMEs are assumed to be isotropically distributed on the stellar surface ($\Theta = \pi/2$). Note that, for the Sun, most CMEs originate in the region around the equator with $\Theta = \pi/3$ (Khodachenko et al., 2006a). However, the larger value of Θ is chosen to obtain an upper limit for f^{c}_{CME}. Thus, for a CME production rate exceeding f^{c}_{CME} with

$$10\,\mathrm{day}^{-1} \leqslant f^{c}_{CME} \leqslant 36\,\mathrm{day}^{-1} \quad (19)$$

one obtains continuous action of CMEs. Note that these values for the critical CME production rate are not much higher than the CME production rate of the present-day Sun at its activity maximum ($f_{CME} \sim 6 \ldots 8\,\mathrm{day}^{-1}$). For this reason, the assumption of a permanent influence of stellar CMEs on a close-in planet appears not to be unrealistic.

The numbers given so far strongly differ from the number of CMEs recorded at the Earth's orbit at 1 AU. The reason for this apparent discrepancy is the fact that only a small fraction of the CMEs reach such large orbital distances. Many solar CMEs could not be tracked by the LASCO instrument on board of SoHO beyond orbital distances of $\approx 0.05\,\mathrm{AU}$ (Khodachenko et al., 2006a). Only about 20% (possibly even less) of all CMEs are strong enough to reach orbital distances of 1 AU and more. Because of the CME geometry, only a certain fraction of these can be seen at a specific location, e.g. at Earth.

During solar maximum, approximately 0.2 CMEs/day are recorded (Wang et al., 2005). Because of the decreasing number of CMEs with distance, the critical CME production rate given by Eq. (18) has to be corrected by a distance-dependent factor for planets at larger orbital distances. However, for extrasolar planets at orbital distances $d \leqslant 0.05\,\mathrm{AU}$, all CMEs have to be taken into account, thus strongly increasing the number of CME collisions when compared to the planets of the solar system. Also, note that stars which are different from the Sun (especially younger stars) may exhibit a stronger CME activity than the Sun.

For close-in planets around stars where the CME occurrence rate exceeds the critical value (i.e. $f_{\mathrm{CME}} > f^{\mathrm{c}}_{\mathrm{CME}}$), the planet can be considered to be under continuous influence of CMEs. In this case the speed and density of the stellar wind around the planet have to be replaced by the CME speed and density. This is based on the assumption that the duration of each CME is long enough, so that its action on a planet can be regarded as the action of a stellar wind with the density and velocity of the CME. The typical duration of a CME is several hours, and the typical reaction time of the magnetosphere is of the order of several minutes. For this reason, this assumption appears reasonable, and n_{CME} and v_{CME} obtained in Section 3.1 can be used analogous to the stellar wind parameters n and v.

4. Size of the magnetosphere

The magnetopause standoff distance R_{s} can be obtained from the pressure equilibrium at the substellar point. This pressure balance includes the stellar wind ram pressure, the stellar wind thermal pressure of electrons and protons and the planetary magnetic field pressure:

$$mnv^2_{\mathrm{eff}} + 2nk_{\mathrm{B}}T = \frac{\mu_0 f_0^2 \mathscr{M}^2}{8\pi^2 R_{\mathrm{s}}^6}. \tag{20}$$

Here, $f_0 = 1.16$ is the form factor of the magnetosphere and includes the magnetic field caused by the currents flowing on the magnetopause (Voigt, 1995; Grießmeier et al., 2004). $\mathscr{M}$ is the planetary magnetic dipole moment, for which a rough estimation can be obtained by simple scaling laws (Farrell et al., 1999; Sánchez-Lavega, 2004; Grießmeier et al., 2004).

The estimated magnetic moment of τ Bootes b, relative to the magnetic moment of Jupiter ($\mathscr{M}_{\mathrm{J}} = 1.56 \times 10^{27}\,\mathrm{A\,m^2}$, see Cain et al., 1995), is given in Table 2, which contains some stellar and planetary data. For the planetary radius, the most probable radius is taken: $R_{\mathrm{p}} = 1.2 R_{\mathrm{J}}$ (Leigh et al., 2003). The planet is assumed to have the minimum mass ($M = 4.4 M_{\mathrm{J}}$). This corresponds to the "light" planet case of Section 5.4.2, wherein we study how strongly the results depend on the assumed planetary parameters. The value for $\mathscr{M}$ was obtained by a procedure similar to that described in Grießmeier et al. (2004). The differences are: (a) the density profile $\rho(r)$ within the planet (described as a polytropic gas sphere) is obtained from the solution of the Lane–Emden equation (Chandrasekhar, 1957; Sánchez-Lavega, 2004). (b) The size of the planetary core r_{c} is found by searching for the value of r where the density $\rho(r)$ becomes large enough for the transition to the liquid-metallic phase (Sánchez-Lavega, 2004). The transition was assumed to occur at a density of $700\,\mathrm{kg/m^3}$, which is consistent with the range of parameters given by Sánchez-Lavega (2004). The average density in the dynamo region is then obtained by averaging the density over the range $0 \leqslant r \leqslant r_{\mathrm{c}}$. (c) We take the geometrical mean of the maximum and minimum result obtained by the different scaling laws. In Section 5.4.1, we study the influence the uncertainty of the magnetic moment has on the results.

For a given planetary orbital distance d, of the different pressure contributions in Eq. (20) only the magnetospheric magnetic pressure is a function of the distance to the planet, while the other factors are constant. Thus, from the pressure equilibrium equation (20) the standoff distance R_{s} is found to be

$$R_{\mathrm{s}} = \left[\frac{\mu_0 f_0^2 \mathscr{M}^2}{8\pi^2 (mnv^2_{\mathrm{eff}} + 2nk_{\mathrm{B}}T)}\right]^{1/6}. \tag{21}$$

Note that in a few cases, especially for planets with very weak magnetic moments and/or subject to dense and fast stellar winds of young stars, Eq. (21) yields standoff distances $R_{\mathrm{s}} < R_{\mathrm{p}}$, where R_{p} is the planetary radius as given in Table 2. In those cases, R_{s} is set equal to R_{p}, because the magnetosphere cannot be compressed to sizes smaller than the planetary radius. Table 1 lists the standoff distances for the different cases. The age of τ Bootes ($t = 2.4\,\mathrm{Gyr}$) was taken from Saffe et al. (2005). Because the uncertainty on the stellar age is considerable, we study the influence of this uncertainty on the results in Section 5.4.3.

It turns out that for the cases treated here, the thermal pressure of the stellar wind has only a limited influence on the resulting R_{s}. This can be checked by repeating the calculation with T set to zero. For example, for τ Bootes b around a star of 2.4 Gyr age, $R_{\mathrm{s}}/R_{\mathrm{p}} = 4.8$ for $T = 0$ instead of $R_{\mathrm{s}}/R_{\mathrm{p}} = 4.6$. The corresponding radio flux (described below) changes by only approximately 10%. However, it has to be noted that this is not clear a priori, and has to be checked for every configuration.

5. Planetary radio flux

5.1. Planetary radio emission in the solar system

In the solar system, it is known that many components of the radio emission of different planets are driven by the solar wind. The power emitted in the Earth's auroral kilometric radiation (AKR), Saturn's kilometric radiation (SKR) and Jupiter's hectometric emission (HOM) were shown to be strongly correlated with solar wind parameters, for example, by Gallagher and D'Angelo (1981),

Desch and Rucker (1983) and Desch and Barrow (1984), respectively. A similar, albeit somewhat weaker correlation was found for other components of Jupiter's radiation, and for some components of Uranus' and Neptune's radiation. An overview is given in the review papers of Rucker (1987) and Zarka (1998). Of special interest to this work is the good correlation of the radio power with the solar wind dynamic pressure nv^2 and solar wind kinetic energy flux nv^3. Such a correlation was found, for example, by Desch and Rucker (1983) and Barrow and Desch (1989) for SKR and HOM, respectively. This correlation will present the starting point for the radio flux model in Section 5.2.

At the same time it is interesting to note that interplanetary shocks created by CMEs are known to trigger strong decametric (DAM) and hectometric (HOM) emission on Jupiter. For example, Prangé et al. (1993) found indications that an event of very strong DAM emission (at a level observed only a few times every year) was triggered by a solar wind disturbance created by a CME. Similarly, Gurnett et al. (2002) found strong HOM radiation triggered by an interplanetary shock observed by the spacecraft Cassini and Galileo. The peak of emitted intensity occurred around the time when the solar wind density reached its maximum. The question of increased planetary radio emission triggered by CMEs is taken up in Section 5.3.3.

5.2. Calculation of exoplanetary radio emission

It is clear that the radio emission of an extrasolar planet can differ considerably from Jupiter's radio emission. First, extrasolar planets in close orbits around their host star are expected to have much smaller magnetic moments because of their low rotation rates (Farrell et al., 1999; Grießmeier et al., 2004). The small rotation rates result from tidal locking. Second, planets at close distances experience a much denser stellar wind. Both these effects have a strong influence on the *average* radio flux. The much higher number of CME events reaching the planet, on the other hand, will change the *peak* flux of a close-in planet as well as the frequency of its occurrence. For active stars, the CME-dominated *peak* radio flux may even replace the *average* radio flux.

The energy emitted in the radio range is estimated in the following way. Observational evidence suggests that the power emitted by radio waves $P_{\rm rad}$ is roughly proportional to the power input $P_{\rm input}$ (Zarka et al., 2001). The input power $P_{\rm input}$ is believed to be either proportional to the total kinetic energy flux of the solar wind protons impacting on the magnetopause (Desch and Kaiser, 1984; Zarka et al., 1997, 2001; Farrell et al., 1999, 2004; Lazio et al., 2004; Stevens, 2005; Grießmeier et al., 2005) or to the magnetic energy flux of the interplanetary magnetic field (Zarka et al., 2001; Farrell et al., 2004; Zarka, 2004). In this work, the kinetic energy model is adopted:

$$P_{\rm rad} \propto P_{\rm input} \propto R_{\rm s}^2 n v_{\rm eff}^3. \tag{22}$$

In the following, this kinetic energy model will be applied to two different situations, namely the case where the energy input is determined by the steady stellar wind (calculated using the Parker-like stellar wind model of Section 2.2) and the case where the energy input is caused by CMEs (with the parameters given in Section 3.1). The total emitted radio power is calculated relative to the respective value for Jupiter:

$$P_{\rm rad} = \left(\frac{R_{\rm s}/R_{\rm p}}{R_{\rm s,J}/R_{\rm J}}\right)^2 \left(\frac{R_{\rm p}}{R_{\rm J}}\right)^2 \left(\frac{n}{n_{\rm J}}\right) \left(\frac{v_{\rm eff}}{v_{\rm eff,J}}\right)^3 P_{\rm rad,J}. \tag{23}$$

Here, $R_{\rm s}/R_{\rm p}$ corresponds to the magnetospheric standoff distance in planetary radii. The emitted power, however, depends on the absolute standoff distance $R_{\rm s}$, see Eq. (22). The values used for Jupiter are the following: $R_{\rm s,J}/R_{\rm J} = 40$ (see Table 1), $n_{\rm J} = 2.0 \times 10^5\,{\rm m}^{-3}$, and $v_{\rm J} = 520\,{\rm km/s}$. $P_{\rm rad,J}$ is the observed radio flux emitted by Jupiter. It is calculated from Zarka et al. (2004). In the following, the *average radio power during periods of high activity* is used with $P_{\rm rad,J} = 2 \times 10^{11}\,{\rm W}$. For comparison, the *peak power* is given by $P_{\rm rad,J} = 10 \times 10^{11}\,{\rm W}$.

The observable flux density Φ_s at a distance s is connected to $P_{\rm rad}$ in the following way (e.g. Farrell et al., 1999; Grießmeier et al., 2005):

$$\Phi = \frac{P_{\rm rad}}{\Omega s^2 \Delta f}, \tag{24}$$

where Ω is the solid angle of the beam. For τ Bootes, $s = 15.6\,{\rm parsec}$. Assuming the emission to be analogous to the dominating contributions of Jupiter's radio emission, we use $\Omega = 1.6\,{\rm sr}$ (Zarka et al., 2004). Δf denotes the emission bandwidth. It is frequently assumed that $\Delta f \propto f_{\rm c}^{\rm max}$, where the maximum cyclotron frequency $f_{\rm c}^{\rm max}$ is determined by the maximum magnetic field strength $B_{\rm p}^{\rm max}$ close to the polar cloud tops (Farrell et al., 1999):

$$f_{\rm c}^{\rm max} = \frac{e B_{\rm p}^{\rm max}}{2\pi m_{\rm e}}. \tag{25}$$

Here, $m_{\rm e}$ and e are the electron mass and charge. The maximum polar magnetic field strength is given by

$$B_{\rm p}^{\rm max} = \frac{\mu_0}{4\pi} \frac{2\mathscr{M}}{R_{\rm p}^3}, \tag{26}$$

where μ_0 is the vacuum permeability and $R_{\rm p}$ is the planetary radius (given in Table 2). The radio spectrum of Jupiter in Fig. 2 shows that the frequently adopted assumption $\Delta f = 0.5 f_{\rm c}^{\rm max}$ is not a good approximation, so that a larger emission bandwidth of $\Delta f = f_{\rm c}^{\rm max}$ is used instead. This leads to the following expression for the flux density at the position of the observer:

$$\Phi_s = \frac{4\pi^2 m_{\rm e} R_{\rm p}^3 P_{\rm rad}}{e \mu_0 \Omega s^2 \mathscr{M}}. \tag{27}$$

Eqs. (23) and (27) differ from Eqs. (2) and (11) of Grießmeier et al. (2005) in three respects: first, because in Eq. (21) the calculation of the standoff distance includes the thermal pressure, $R_{\rm s}$ cannot be simply expressed by the

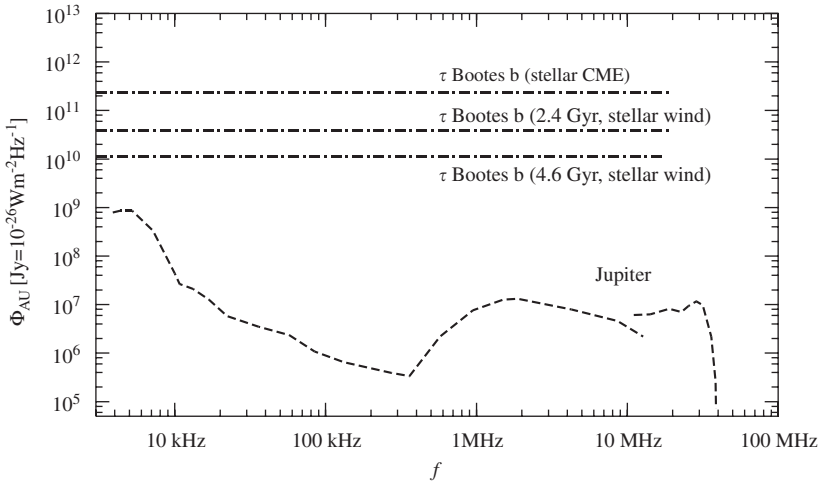

Fig. 2. Radio flux expected for a planet similar to τ Bootes b around stars of 2.4 and 4.6 Gyr age. Both the radio flux energized by the steady stellar wind and that triggered by CME-like stellar coronal mass ejections are compared to the average radio flux of Jupiter during periods of high activity (Zarka et al., 1995, 2004). All flux values are normalized to a distance of 1 AU. Note that for τ Bootes b, emission takes place only for frequencies $f \leqslant f_c^{\max} = 10.5$ MHz, whereas it extends to considerably higher frequencies for Jupiter.

planetary magnetic moment $\mathscr{M}$. Second, the assumption of a distance-independent stellar wind velocity is avoided. Because of mass conservation, this also means that the density profile cannot be written as $n = n_0/d^2$. In Eq. (23), the dependence on orbital distance is contained in the variables $v(d)$ and $n(d)$. Third, the radio emission is assumed to have a bandwidth of $\Delta f = f_c$ rather than $\Delta f = 0.5 f_c$.

5.3. Radio emission under different stellar wind conditions: comparison

In Sections 2.5 and 3.1, it was shown how the plasma parameters can be obtained for the steady-state stellar wind and for stellar CMEs. Inserting these parameters in Eqs. (23) and (27), the expected radio flux can be calculated for the different situations. The planet τ Bootes b will be used as example, and the case of the planet τ Bootes b around a star of 2.4 Gyr age is regarded as the reference case.

Table 1 shows the emitted radio power $P_{\rm rad}$ and the flux densities $\Phi_{\rm AU}$ (normalized to 1 AU) and Φ_s (for an observer at a distance s) for the different cases: the case of Jupiter (shown for comparison), the reference case (REF), stellar wind-driven radio emission obtained with the simplified stellar wind model (SSW2.4), stellar wind-driven radio emission for a star of a different age (SW1.0, SW2.4 and SW4.6) (updating Grießmeier et al., 2005) and magnetospheric radio emission driven by a strong stellar CME (case CME) (updating Grießmeier et al., 2006b). Note that any emission below ~10 MHz will not be detectable on Earth because it cannot propagate through the Earth's ionosphere ("ionospheric cutoff").

5.3.1. Influence of the stellar wind model

To demonstrate the importance of a stellar wind model which takes into account the orbital distance, the results obtained with the Parker-like stellar wind model of Section 2.1 can be compared to the corresponding values found using a more simplified stellar wind model.

For this simplified stellar wind model, the stellar wind velocity of a 2.4 Gyr old star at 1 AU is calculated as $v = 560$ km/s. Correcting for the orbital motion of the planet, we obtain $v_{\rm eff} = 580$ km/s. The density at the location of the planet (i.e. at 0.0489 AU) is found by projecting the stellar wind density at 1 AU (4.8×10^7 m^{-3}) to the planetary orbit using the relation $n \propto d^{-2}$. This results in a value of $n = 2.0 \times 10^{10}$ m^{-3}. Inserting these values into Eqs. (23) and (27), one obtains the radio flux of the case SSW2.4 in Table 1. This flux is about a factor of five above that obtained with the Parker-like stellar wind model, the SW2.4 case of Table 1. This shows that the planetary radio flux is overestimated when the radial dependence of the stellar wind velocity is discarded. At the same time it is important to use $v_{\rm eff}$ rather than v, because the orbital velocity can be of the same order of magnitude as the stellar wind velocity.

5.3.2. Influence of the stellar system age

As was already pointed out by Stevens (2005) and Grießmeier et al. (2005), the planetary radio emission is a function of the age of the stellar system. The reason is that the stellar wind velocity and density are functions of the stellar system age, as described in Section 2.3. The influence of the stellar system age is shown in Table 1 (cases SW2.4 and SW4.6). In this example, the difference between the radio flux of planets around young (2.4 Gyr age) and old (4.6 Gyr age) stars is approximately a factor of four. This is also shown in Fig. 2. Note that the age of τ Bootes was estimated to be approximately 1.0 Gyr by Fuhrmann et al. (1998), whereas more recently Saffe et al. (2005) gave an age of approximately 2.4 Gyr. This value was adopted for this work. With this new value, the radio flux expected

from τ Bootes b is reduced when compared to previous estimations. While the two age determinations seem considerably different (Table 1 shows that the expected radio flux is much higher for the SW1.0 case than for SW2.4), these ages are still compatible within the error-bars. This shows how important it is to know the stellar age as precisely as possible (see also Section 5.4.3).

5.3.3. Influence of stellar CMEs

Table 1 also compares the planetary radio fluxes connected to the steady stellar wind (cases SW1.0, SW2.4 and SW4.6) to that triggered by strong stellar CMEs (case CME). One can see that in the strong CME case, the radio flux is considerably higher than for a stellar wind of a 4.6 or a 2.4 Gyr old star. It is comparable to the radio flux energized by the stellar wind of a young star (approx. 1.0 Gyr).

In Fig. 2, the expected planetary radio flux Φ_{AU} for radio emission driven by the stellar wind of 4.6 and 2.4 Gyr old stars are compared to the radio emission driven by a strong CME. For comparison, the dashed line shows the radio spectrum of Jupiter. One can clearly see that for a close-in extrasolar planet around a star of 4.6 Gyr age, radio emission driven by a CME is much stronger than solar wind-driven emission. In the case presented here, both emissions differ by a factor of almost 20. The CME-driven radio flux is still considerably higher than the stellar wind-driven flux when $P_{rad,J}$ is set equal to 11×10^{11} W instead of 2.1×10^{11} W (i.e. using the *peak* flux instead of the *average value during periods of high activity*). This comparison shows that CMEs have to be taken into account when discussing exoplanetary radio emission.

5.4. Errors and uncertainties

With all different factors and approximations used in the radio flux estimation, one might wonder how reliable the results and conclusions are. To study this, we examine different sources of uncertainty and calculate the range of results for each error. The ranges of possible results are shown in Table 3. The first row of Table 3 represents the reference case; the other rows are discussed in detail below. This comparison will show which uncertainties dominate the total error of the result.

Note that the relative importance of the uncertainties need not be the same for all planets. When other planets than τ Bootes b are studied, a different error may dominate. For example, the effect of the error-bar of the stellar age becomes less important for older stars.

Also note that the total error cannot simply be obtained by adding all individual errors. For example, the case constructed by taking the maximum value allowed by each single source of uncertainty *at the same time* is an extremely unlikely case, and does not correspond to a 1σ error.

5.4.1. Uncertainty of magnetic moment

Presently, the magnetic moment of extrasolar planets is not an observable quantity. Rather, it is estimated by using different scaling laws. The magnetic moment of the reference case ($\mathcal{M} = 0.76\,\mathcal{M}_J$) was obtained by taking the geometrical mean of the maximum and minimum value obtained by different scaling laws. Here, the maximum and minimum values are considered separately ($0.48\,\mathcal{M}_J \leqslant \mathcal{M} \leqslant 1.2\,\mathcal{M}_J$).

In addition, we do not expect tidal interaction to perfectly synchronize the planetary rotation to its orbit. Thermal atmospheric tides resulting from stellar heating can drive planets away from synchronous rotation (Showman and Guillot, 2002; Correia et al., 2003; Laskar and Correia, 2004). Showman and Guillot (2002) estimated the deviation from synchronous rotation resulting from atmospheric tides for a typical Hot Jupiter. As an upper limit, it was found that the error introduced for the rotation rate by this effect could be of the same order of magnitude as the value itself. For this reason, we allow the planetary rotation rate to be between zero and double the value given by synchronous rotation. This leads to planetary magnetic dipole moments between $0 \leqslant \mathcal{M} \leqslant 1.7\,\mathcal{M}_J$. However, emissions below 10 MHz cannot be observed from the ground, and magnetic moments resulting in such low-frequency emissions are not of interest. Therefore, we study the range of $0.73 \leqslant \mathcal{M} \leqslant 1.7\,\mathcal{M}_J$.

Table 3 (second row) shows that, with this range of magnetic moments, we find only little difference for the

Table 3
Age t, planetary radius and mass, expected planetary magnetic moment $\mathcal{M}$, stellar wind parameters (density, velocity and temperature), magnetospheric standoff distances R_s (in planetary radii), estimated flux density at distance s (Φ_s), and maximum emission frequency f_c^{max} for different cases

Planet	Case	t (Gyr)	R_p (R_J)	M_p (M_J)	$\mathcal{M}$ ($\mathcal{M}_J$)	n (10^{10} m^{-3})	v_{eff} (km/s)	T (MK)	R_s (R_p)	Φ_s (mJy)	f_c^{max} (MHz)
τ Bootes b	Reference case	2.4	1.2	4.4	0.76	4.9	280	1.4	4.6	3.9	10.5
τ Bootes b	Var. $\mathcal{M}$	2.4	1.2	4.4	0.73[a] ... 1.7	4.9	280	1.4	4.5 ... 6.0	3.0 ... 3.9	10[a] ... 24
τ Bootes b	Var. R_p, M_p	2.4	1.2 ... 1.58	4.4 ... 10.0	0.76 ... 1.66	4.9	280	1.4	4.3 ... 4.8	3.9 ... 7.2	8.7 ... 12.3
τ Bootes b	Var. t	1.3 ... 3.1	1.2	4.4	0.76	3.3 ... 13	250 ... 390	1.1 ... 2.0	3.5 ... 5.1	2.2 ... 16	10.5
τ Bootes b	Var. age model	2.4	1.2	4.4	0.76	3.3 ... 7.2	280	1.4	4.3 ... 4.9	3.0 ... 5.0	10.5
τ Bootes b	Var. n_{CME}	–	1.2	4.4	0.76	0.51 ... 6.1	530	2	3.7 ... 5.5	3.8 ... 20	10.5

In each row (except for the first, which gives the reference case) the uncertainty of one specific parameter and the resulting implications for the radio flux estimation are given. *Note*: [a] see text.

estimated radio flux. However, for the emission frequency, a considerable difference is found between maximum and minimum value.

5.4.2. Uncertainty of planetary mass and radius

For most known exoplanets, only the lower limit for the planetary mass is known ($M_p \sin i$, where i is the orbital inclination relative to the observer). Also, for most exoplanets, the planetary radius is unknown. For example, for the planet τ Bootes b, $M_p \sin i = 4.38 M_J$ (Leigh et al., 2003), and R_p is presently not accessible to measurements.

To study the effect of this uncertainty on the radio flux estimation, three different models are considered for τ Bootes b. Theoretical models by Burrows et al. (2000) yield an upper limit for the radius. This upper limit is $1.58 R_J$ for a planetary mass of $7 M_J$ and $1.48 R_J$ for $10 M_J$. The most probable radius seems to be $1.2 R_J$ (Leigh et al., 2003). Because of this uncertainty, we calculate the magnetic moment for three different cases: a relatively "light" planet ($M = 4.4 M_J$ and $R = 1.2 R_J$), a "medium" planet ($M = 7.0 M_J$ and $R = 1.58 R_J$) and a "heavy" planet ($M = 10.0 M_J$ and $R = 1.48 R_J$). For each of these three model cases, the magnetic moment $\mathscr{M}$ is calculated, which then is used for the radio flux calculation.

The third row of Table 3 shows the minimum and maximum values obtained with these three planetary models. The difference in radio flux is lower than a factor of two, and the maximum emission frequency differs by approximately 40%. Note that emission frequencies below 10 MHz are not observable from the ground; they are included here to facilitate the comparison of the relative importance of the different sources of uncertainty.

5.4.3. Uncertainty of stellar age

Unfortunately, stellar ages are not determined very precisely. For example, the isochron age of τ Bootes is estimated to lie in the range 1.3 ... 3.1 Gyr, with 2.4 Gyr as the most likely value (Saffe et al., 2005).

The impact of this uncertainty on the radio flux estimation is shown in Table 3 (fourth row). For the case of τ Bootes, the flux density varies by a factor of seven.

Note that the relevance of this uncertainty is determined by the stellar age. The younger the star, the stronger the difference in v and n (and thus also in the resulting radio flux Φ_s) generated by a given age uncertainty Δt.

5.4.4. Uncertainty of the stellar wind age model

The procedure followed to obtain the equation used to determine the stellar wind density as a function of stellar age relies on several approximations, leading to the errorbars indicated in Eq. (7). In the following, v is assumed to be correct, but the error in n is considered. The fifth row of Table 3 shows that, in the case of τ Bootes, this uncertainty introduces variations of less than a factor two.

Similar to the error introduced by the uncertainty in the stellar age, the relevance of this uncertainty may be very different for different planets. In fact, it is zero for stars of 4.6 Gyr age and increases with increasing deviation of t from that value.

5.4.5. Uncertainties for the CME case

In Section 3.1, two different types of CMEs were discussed, namely strong and weak CMEs. In Section 5.3.3 and Fig. 2, the strong CME case was considered. Here, we now examine how the results change if the weak CME case is taken instead.

From Table 3 (last row) it can be seen that weak and strong CMEs differ quite considerably, leading to differences of a factor of five in the radio flux estimation. Because in the solar system both types of CME exist, strong CME-triggered radio emission may still happen, but with a reduced occurrence rate. Note that even weak CMEs lead to a radio flux approximately three times as high as that expected in the case of 4.6 Gyr old stellar wind (cf. Table 1).

5.4.6. Discussion of uncertainties

The detailed comparison of different uncertainties shows that, for the maximum emission frequency $f_c^{\max}$, the uncertainty of the planetary magnetic moment dominates. For the radio flux expected on Earth, Φ_s, the uncertainty of the planetary age dominates. Especially for planets around young stars, this factor has to be kept in mind.

The analysis of errors also shows that, despite the uncertainties involved, the conclusions of Section 5.3 are still valid, as the age of the system clearly is an important factor, the use of a distance-dependent stellar wind model makes a significant difference, and CMEs may potentially lead to very strong radio emission.

6. Conclusion

Different ways of describing the stellar wind of exoplanetary host stars were discussed. It was shown that in order to correctly estimate the planetary radio flux, a simplified stellar wind model with constant velocity may not be sufficient. Because, for close-in exoplanets the stellar wind velocity is considerably lower than it is in the quasi-asymptotic velocity regime reached at larger distances, it is necessary to use a model with a distance-dependent stellar wind velocity. It was also shown that a Parker-like stellar wind model is sufficient to adequately describe the stellar wind of the star τ Bootes, and that the more refined stellar wind model by Weber and Davis is not required. Also, the influence of the planetary orbital velocity has to be taken into account.

It was shown that the stellar wind emanating from a young star is capable of driving much stronger planetary radio emission than, for example, the solar wind. The gain in radio flux strongly depends on the age of the stellar system; for τ Bootes b, it is approximately a factor of four.

Planetary radio emission triggered by stellar CMEs may be much stronger than radio emission supplied by the kinetic energy of the steady stellar wind. Collisions of

stellar CMEs with close-in planets are expected to happen much more frequently than with planets at larger orbital distances. For this reason, it is possible that CMEs replace the stellar wind not only sporadically, but that the planet is continuously under the influence of CMEs. Such a situation would lead to a strongly enhanced planetary radio flux, similar to that of a planet around a young star.

These effects confirm that not only the planetary parameters must be considered when calculating the expected radio fluxes for different planets. Parameters like the stellar mass, radius or age directly influence the stellar wind environment of the planet, and thus are responsible for the amount of energy available for planetary radio emission. These factors have to be taken into account when comparing the radio fluxes expected for different exoplanets, or when comparing the expected radio fluxes to past observation attempts (as done, e.g. by Grießmeier et al., 2006a). This could also be of importance when establishing target lists for future observations, suggesting that young, flaring stars, for which frequent CME-like effects are expected, might be interesting targets.

Acknowledgments

We would like to thank both referees for their useful comments and suggestions. Part of this work was performed during a stay of J.-M.G. at the Institut für Weltraumforschung, Graz, which is gratefully acknowledged.

References

Barrow, C.H., Desch, M.D., 1989. Solar wind control of Jupiter's hectometric radio emission. Astron. Astrophys. 213, 495–501.

Burrows, A., Guillot, T., Hubbard, W.B., Marley, M.S., Saumon, D., Lunine, J.I., Sudarsky, D., 2000. On the radii of close-in giant planets. Astrophys. J. 534, L97–L100.

Cain, J.C., Beaumont, P., Holter, W., Wang, Z., Nevanlinna, H., 1995. The magnetic bode fallacy. J. Geophys. Res. 100 (E5), 9439–9454.

Chandrasekhar, S., 1957. An Introduction to the Study of Stellar Structure. Dover Books on Astronomy and Astrophysics. Dover, New York.

Collier Cameron, A., Jianke, L., 1994. Magnetic braking of G and K dwarfs without core-envelope decoupling. Mon. Not. R. Astron.Soc 269, 1099–1111.

Correia, A.C.M., Laskar, J., de Surgy, O.N., 2003. Long-term evolution of the spin of Venus I. Theory. Icarus 163, 1–23.

Desch, M.D., Barrow, C.H., 1984. Direct evidence for solar wind control of Jupiter's hectometer-wavelength radio emission. J. Geophys. Res. 89 (A8), 6819–6823.

Desch, M.D., Kaiser, M.L., 1984. Predictions for Uranus from a radiometric Bode's law. Nature 310, 755–757.

Desch, M.D., Rucker, H.O., 1983. The relationship between Saturn kilometric radiation and the solar wind. J. Geophys. Res. 88 (A11), 8999–9006.

Erkaev, N.V., Penz, T., Lammer, H., Lichtenegger, H.I.M., Biernat, H.K., Wurz, P., Grießmeier, J.-M., Weiss, W.W., 2005. Plasma and magnetic field parameters in the vicinity of short-periodic giant exoplanets. Astrophys. J. Suppl. Ser. 157, 396–401.

Farrell, W.M., Desch, M.D., Zarka, P., 1999. On the possibility of coherent cyclotron emission from extrasolar planets. J. Geophys. Res. 104 (E6), 14025–14032.

Farrell, W.M., Lazio, T.J.W., Zarka, P., Bastian, T.J., Desch, M.D., Ryabov, B.P., 2004. The radio search for extrasolar planets with LOFAR. Planet. Space Sci. 52 (15), 1469–1478.

Fuhrmann, K., Pfeiffer, M.J., Bernkopf, J., 1998. F- and G-type stars with planetary companions: ν Andromedae, ρ^1 Cancri, τ Bootis, 16 Cygni and ρ Coronae Borealis. Astron. Astrophys. 336, 942–952.

Gallagher, D.L., D'Angelo, N., 1981. Correlations between solar wind parameters and auroral kilometric radiation intensity. Geophys. Res. Lett. 8 (10), 1087–1089.

Grießmeier, J.-M., Stadelmann, A., Penz, T., Lammer, H., Selsis, F., Ribas, I., Guinan, E.F., Motschmann, U., Biernat, H.K., Weiss, W.W., 2004. The effect of tidal locking on the magnetospheric and atmospheric evolution of "Hot Jupiters". Astron. Astrophys. 425, 753–762.

Grießmeier, J.-M., Motschmann, U., Mann, G., Rucker, H.O., 2005. The influence of stellar wind conditions on the detectability of planetary radio emissions. Astron. Astrophys. 437, 717–726.

Grießmeier, J.-M., Motschmann, U., Glassmeier, K.-H., Mann, G., Rucker, H.O., 2006a. The potential of exoplanetary radio emissions as an observation method. In: Arnold, L., Bouchy, F., Moutou, C. (Eds.), Tenth Anniversary of 51 Peg-b: Status of and Prospects for Hot Jupiter Studies. Platypus Press, pp. 259–266. URL: ⟨http://www.obs-hp.fr/www/pubs/Coll51Peg/proceedings.html⟩.

Grießmeier, J.-M., Motschmann, U., Khodachenko, M., Rucker, H.O., 2006b. The influence of stellar coronal mass ejections on exoplanetary radio emission. In: Rucker, H.O., Kurth, W.S., Mann, G. (Eds.), Planetary Radio Emissions VI. Austrian Academy of Sciences Press, Vienna, pp. 571–579.

Guinan, E.F., Ribas, I., 2002. Our changing sun: the role of solar nuclear evolution and magnetic activity on Earth's atmosphere and climate. In: Montesinos, B., Gimenez, A., Guinan, E.F. (Eds.), The Evolving Sun and its Influence on Planetary Environments. ASP Conference Series, vol. 269. pp. 85–107.

Gurnett, D.A., Kurth, W.S., Hospodarsky, G.B., Persoon, A.M., Zarka, P., Lecacheux, A., Bolton, S.J., Desch, M.D., Farrell, W.M., Kaiser, M.L., Ladreiter, H.-P., Rucker, H.O., Galopeau, P., Louarn, P., Young, D.T., Pryor, W.R., Dougherty, M.K., 2002. Control of Jupiter's radio emission and aurorae by the solar wind. Nature 415, 985–987.

Khodachenko, M.L., Ribas, I., Lammer, H., Grießmeier, J.-M., Leitner, M., Selsis, F., Eiroa, C., Hanslmeier, A., Biernat, H.K., Farrugia, C.J., Rucker, H.O., 2006a. CME activity of low mass M stars as an important factor for the habitability of terrestrial exoplanets. Part I: CME impact on expected magnetospheres of Earth-like exoplanets in close-in habitable zones. Astrobiology, submitted for publication.

Khodachenko, M.L., Lammer, H., Lichtenegger, H.I.M., Langmayr, D., Erkaev, N.V., Grießmeier, J.-M., Leitner, M., Penz, T., Biernat, H.K., Motschmann, U., Rucker, H.O., 2006b. Mass loss of "Hot Jupiters"—Implications for CoRoT discoveries. Part I: the importance of magnetospheric protection of a planet against ion loss caused by Coronal Mass Ejections. Planet. Space. Sci., 2006, this issue, doi:1016/j.pss.2006.07.010.

Lammer, H., Ribas, I., Grießmeier, J.-M., Penz, T., Hanslmeier, A., Biernat, H.K., 2004. A brief history of the solar radiation and particle flux evolution. Hvar Obs. Bull. 28, 139–155.

Lara, A., González-Esparza, J.A., Gopalswamy, N., 2004. Characteristics of coronal mass ejections in the near Sun interplanetary space. Geofis. Int. 43 (1), 75–82.

Laskar, J., Correia, A.C.M., 2004. The rotation of extra-solar planets. In: Beaulieu, J.-P., Lecavelier des Etangs, A., Terquem, C. (Eds.), Extrasolar Planets: Today and Tomorrow. ASP Conference Series, vol. 321. pp. 401–410.

Lazio, T.J.W., Farrell, W.M., Dietrick, J., Greenless, E., Hogan, E., Jones, C., Hennig, L.A., 2004. The radiometric Bode's law and extrasolar planets. Astrophys. J. 612, 511–518.

Leigh, C., Collier Cameron, A., Horne, K., Penny, A., James, D., 2003. A new upper limit on the reflected starlight from τ Bootis b. Mon. Not. R. Astron. Soc. 344, 1271–1282.

Mann, G., Jansen, F., MacDowall, R.J., Kaiser, M.L., Stone, R.G., 1999. A heliospheric model and type III radio bursts. Astron. Astrophys. 348, 614–620.

Newkirk Jr., G., 1980. Solar variability on time scales of 10^5 years to $10^{9.6}$ years. In: Pepin, R.O., Eddy, J.A., Merrill, R.B. (Eds.), The Ancient Sun: Fossil Record in the Earth, Moon and Meteorites. pp. 293–320.

Parker, E.N., 1958. Dynamics of the interplanetary gas and magnetic fields. Astrophys. J. 128, 664–676.

Prangé, R., Zarka, P., Ballester, G.E., Livengood, T.A., Denis, L., Carr, T., Reyes, F., Bame, S.J., Moos, H.W., 1993. Correlated variations of UV and radio emissions during an outstanding Jovian auroral event. J. Geophys. Res. 98 (E10), 18779–18791.

Preusse, S., 2006. Szenarien der Plasmawechselwirkung in kurzperiodischen extrasolaren Planetensystemen. Ph.D. Thesis, Technische Universität Braunschweig, Copernicus-GmbH, Katlenburg-Lindau, ISBN 3-936586-48-9.

Preusse, S., Kopp, A., Büchner, J., Motschmann, U., 2005. Stellar wind regimes of close-in extrasolar planets. Astron. Astrophys. 434, 1191–1200.

Prölss, G.W., 2004. Physics of the Earth's Space Environment. Springer, Berlin.

Rucker, H.O., 1987. Solar wind influence on non-thermal planetary radio emission. Ann. Geophys. 5A (1), 1–11.

Saffe, C., Gómez, M., Chavero, C., 2005. On the ages of exoplanet host stars. Astron. Astrophys. 443, 609–626.

Sánchez-Lavega, A., 2004. The magnetic field in giant extrasolar planets. Astrophys. J. 609, L87–L90.

Schwenn, R., 1990. Large-scale structure of the interplanetary medium. In: Schwenn, R., Marsch, E. (Eds.), Physics of the Inner Heliosphere, vol. 1. Springer, Berlin, pp. 99–181 (Chapter 3).

Showman, A.P., Guillot, T., 2002. Atmospheric circulation and tides of "51 Pegasus b-like" planets. Astron. Astrophys. 385, 166–180.

Stevens, I.R., 2005. Magnetospheric radio emission from extrasolar giant planets: the role of the host stars. Mon. Not. R. Astron. Soc. 356, 1053–1063.

Voigt, G.-H., 1995. Magnetospheric configuration. In: Volland, H. (Ed.), Handbook of Atmospheric Electrodynamics, vol. II. CRC Press, Boca Raton, FL, pp. 333–388 (Chapter 11).

Wang, C., Du, D., Richardson, J.D., 2005. Characteristics of the interplanetary coronal mass ejections in the heliosphere between 0.3 and 5.4 AU. J. Geophys. Res. 110 (A10), A10107.

Weber, E.J., Davis Jr., L., 1967. The angular momentum of the solar wind. Astrophys. J. 148, 217–227.

Wood, B.E., 2004. Astrospheres and solar-like stellar winds. Living Rev. Sol. Phys. 1, 2. URL: ⟨http://www.livingreviews.org/lrsp-2004-2⟩ (accessed on 11 October 2005).

Wood, B.E., Müller, H.-R., Zank, G.P., Linsky, J.L., 2002. Measured mass-loss rates of solar-like stars as a function of age and activity. Astrophys. J. 574, 412–425.

Wood, B.E., Müller, H.-R., Zank, G.P., Linsky, J.L., Redfield, S., 2005. New mass-loss measurements from astrospheric Lyα absorption. Astrophys. J. 628, L143–L146.

Zarka, P., 1998. Auroral radio emissions at the outer planets: observations and theories. J. Geophys. Res. 103 (E9), 20159–20194.

Zarka, P., 2004. Non-thermal radio emissions from extrasolar planets. In: Beaulieu, J.-P., Lecavelier des Etangs, A., Terquem, C. (Eds.), Extrasolar Planets: Today and Tomorrow. ASP Conference Series, vol. 321. pp. 160–169.

Zarka, P., Pedersen, B.M., Lecacheux, A., Kaiser, M.L., Desch, M.D., Farrell, W.M., Kurth, W.S., 1995. Radio emissions from Neptune. In: Cruikshank, D.P. (Ed.), Neptune and Triton. University of Arizana Press, Tucson, pp. 341–387.

Zarka, P., Queinnec, J., Ryabov, B.P., Ryabov, V.B., Shevchenko, V.A., Arkhipov, A.V., Rucker, H.O., Denis, L., Gerbault, A., Dierich, P., Rosolen, C., 1997. Ground-based high sensitivity radio astronomy at decameter wavelengths. In: Rucker, H.O., Bauer, S.J., Lecacheux, A. (Eds.), Planetary Radio Emissions IV. Austrian Academy of Sciences Press, Vienna, pp. 101–127.

Zarka, P., Treumann, R.A., Ryabov, B.P., Ryabov, V.B., 2001. Magnetically-driven planetary radio emissions and application to extrasolar planets. Astrophys. Space Sci. 277, 293–300.

Zarka, P., Cecconi, B., Kurth, W.S., 2004. Jupiter's low frequency radio spectrum from Cassini/radio and plasma wave science (RPWS) absolute flux density measurements. J. Geophys. Res. 109 (A09), A09S15.